ACI STRUCTURAL JOURNAL TECHNICAL PAPER

Title No. 115-S132

Bond Strength of Reinforcing Bars with Varying Encapsulation Qualities

by Pasquale Basso Trujillo, Marc Jolin, Bruno Massicotte, and Benoît Bissonnette

*The encapsulation quality of reinforcing bars represents a common concern among structural engineers when shotcrete structures are designed. Because little scientific information is available regarding the potential bond strength reduction of bars with adjacent defects along their length, ASTM A944-10 "beam-end" specimens with different encasement qualities were tested. To limit the size variability of voids when spraying, voids were created using silicone inserts, which also made it possible to control their exact size and position. Artificial voids were encased with a placed shotcrete mixture and transversal lengths of up to 30% of the bars' perimeter were investigated. A low water-binder ratio (*w/b*) was employed to guarantee an insignificant bleeding capacity of the mixture as is commonly observed in shotcrete. The results support previous investigations by showing that transversal void lengths beyond 20% induce a considerable change in the slope of the stress-slip curve and an important reduction of the ultimate bond stress.*

Keywords: artificial voids; beam end; bond strength; encapsulation; hypothesis testing; shotcrete; sprayed concrete; voids.

INTRODUCTION

Ever since the 1933 Long Beach earthquake in California, the use of shotcrete as a way to retrofit structural elements has rapidly increased in North America.[1] Its use has grown so quickly that nowadays, it is not unusual to see tunnel linings,[2] domes,[3] shear walls,[4] or even columns[5] and girders[2] being entirely built with shotcrete. The main reasons for this include the small amount (if any) of formwork needed and the ability to build structural elements of almost any shape, which often results in considerable time and cost savings. However, using the current design criteria may not be completely adequate for reinforced shotcrete elements because of the different placement processes between shotcrete and cast-in-place concrete. In particular, a recurring concern among structural engineers has been the possibility to encounter voids or entrapped aggregates (usually referred to as sand pockets) behind reinforcing bars. In wet-mix shotcrete, such defects are generally caused by the use of excessive set-accelerating admixtures and in dry-mix shotcrete by the inadequate selection of the water content by the nozzlemen. However, imperfections can be caused with the use of both processes if inadequate placement techniques are used. In reality, the concern regarding the encapsulation quality of reinforcement is widespread and covers many aspects from the design of structures to the evaluation of cores taken from preconstruction panels. Up until now, this issue has been addressed only for evaluation of shotcrete quality and not design. The approach has been to quantitatively characterize the size of the voids observed in cores[6] and then determine if the individual/crew is sufficiently experienced to place good-quality shotcrete. Unfortunately, the limits determining what is "acceptable" and "unacceptable" have been chosen empirically. An alternative and perhaps a more advantageous way to deal with both the evaluation and the design might be to establish a void size threshold (based on the bond strength performance of bars) beyond which design criteria applicable specifically for shotcrete should be adopted. Accordingly, the evaluation of cores could be relaxed knowing that preventive measures were taken during the "design phase" to overcome the structural effect of such imperfections. The development length of reinforcing bars required to be computed by North American design codes[7,8] may represent a suitable parameter to be adapted in such situations. However, a considerable amount of scientific information regarding the effect of different void sizes on the bond strength of a bar is lacking and would be needed for this purpose.

Early results within this research project using "pullout" specimens[9] have shown that the height of the voids behind reinforcing bars contributes little to the reduction of the bond strength and that a void's transversal length in contact with the bar (referred to as the unbonded perimeter) exceeding approximately 20% of the bar's perimeter represent the onset of a significant bond reduction and a change of failure mode from splitting to pullout. In that investigation, artificial voids created with silicone inserts and encased with a placed shotcrete mixture were used to overcome the difficulty to obtain specific void sizes and limit their size variability when spraying. A statistical comparison between the results obtained with such type of specimens and equivalent ones made with dry-mix shotcrete showed that the ultimate loads were statistically equivalent between them and that, although the shape of their load-slip curve differed, artificial voids represented a valuable method to ultimately set rational evaluation and design criteria.[9]

In this research, the ASTM A944-10[10] "beam-end" specimens were used to study the impact of defects on the bond behavior of reinforcing bars. This type of specimen is advantageous because it accurately recreates the stress distribution around tensioned bars of most structural elements.[11] However, because spraying specimens in the laboratory to obtain imperfect encapsulation qualities has proven to be a difficult task, the specimens were cast-in-place using a self-consolidating concrete (SCC) mixture poured by gravity

ACI Structural Journal, V. 115, No. 6, November 2018.
MS No. S-2017-412.R1, doi: 10.14359/51702415, was received November 1, 2017, and reviewed under Institute publication policies.

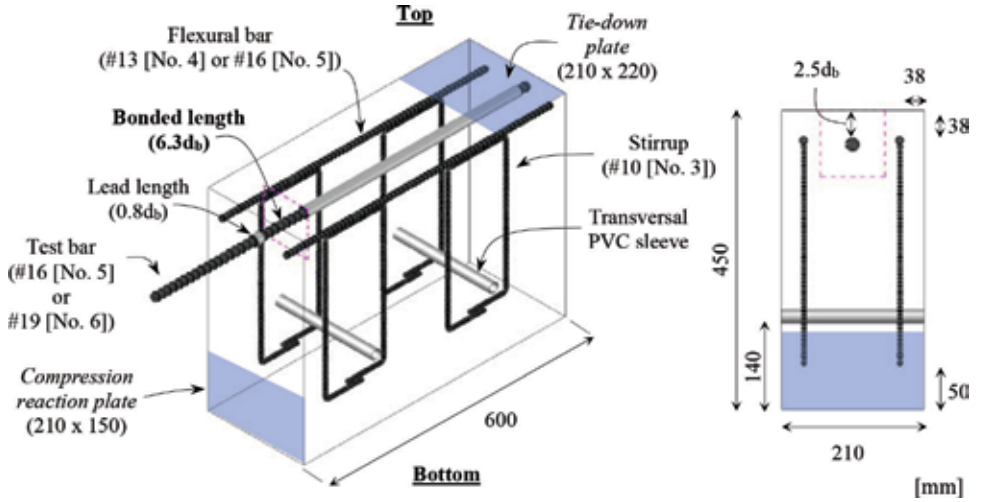

Fig. 1—ASTM A944-10 "beam-end" specimen. (Note: 25.4 mm = 1 in.)

into the molds. As in the past investigation,[9] the voids were recreated using artificial voids. This was done to obtain the most representative mechanical properties possible of typical shotcrete whilst minimizing the bleeding capacity of the mixture and to obtain a "reliably imperfect" bar-concrete interface with known void sizes.

RESEARCH SIGNIFICANCE

This experimental investigation intends to broaden knowledge regarding the bond strength reduction caused by the possible presence of voids specifically behind reinforcing bars created with improperly placed shotcrete. Ultimately, the information will serve to develop reliable guidelines for the design of shotcrete structures (in particular for the computation of the development length of bars in tension specified by North American design codes[7,8]) and for the evaluation of concrete cores as the values in existing tools were chosen subjectively and not based on the actual bond behavior of specimens tested in the laboratory.

EXPERIMENTAL INVESTIGATION

Test specimens

"Beam-end" specimens were built in accordance with the ASTM A944-10 standard[10] and consisted of 210 x 600 x 450 mm (8.3 x 23.6 x 17.7 in.) prisms with a single test bar passing through a polyvinyl chloride (PVC) sleeve at the loaded end (called the lead length) and a second sleeve at the unloaded end as seen in Fig. 1. The bonded length of the test bar was therefore controlled by these bond breaking sleeves. Test bars of 15.9 and 19.1 mm (5/8 and 6/8 in.) nominal diameter d_b were tested and placed with their longitudinal ribs facing the sides of the forms. The lead length and the bonded length were set as $0.8d_b$ and $6.3d_b$, respectively, for all specimens. The flexural bars were 12.7 and 15.9 mm (4/8 and 5/8 in.) in nominal diameter for each of the test bars, respectively. The flexural bars (9.5 or 12.7 mm [3/8 or 4/8 in.], depending on the test bar size) and the stirrups (9.5 mm [3/8 in.] for all specimens) are required by the standard to assure proper behavior in flexure and in shear. Additional PVC sleeves were placed transversally (with respect to the test bar) in between the stirrups so they could be used to move the specimens after being stripped. The concrete

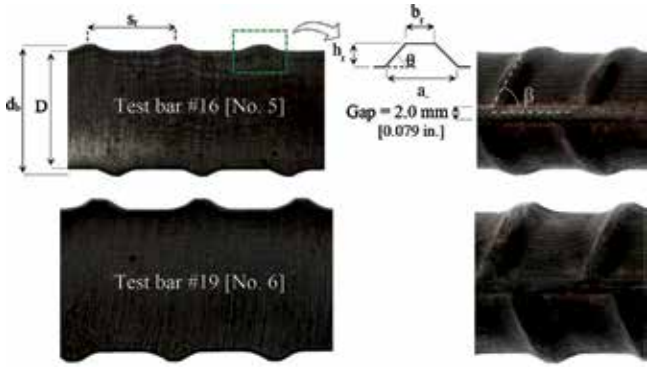

Fig. 2—Longitudinal cut with geometry nomenclature of No. 16 (No. 5) and No. 19 (No. 6) bars.

cover of the test bars was set to $2.5d_b$ for all specimens, which represents the cover beyond which the bond strength does not increase if a pullout failure occurs (as this type of failure become more predominant over a splitting failure as the concrete cover increases).[12,13] Specimens were cast in detachable wooden panels held together by steel threaded rods. After the test bar and its front and back sleeves were secured in place, the forms were carefully oiled. Subsequently, the flexural bars and the stirrups (attached together using cable ties) were placed inside the forms and lastly, the transversal PVC sleeves were installed. This sequence guaranteed a wider space between the form and the test bar to avoid staining the bars with the form release agent. Prior to casting, all of the joints and holes in the formwork holding the bars and PVC sleeves in place were caulked with silicone. Twenty-four hours after, the specimens were stripped and were cured for 1 week using wet burlap.

Reinforcing bars

The reinforcing bars came from the same heat of steel and complied with the ASTM A615/A615M-16 standard.[14] Their mechanical properties were averaged from three specimens and tested in accordance with ASTM A370-17.[15] Additional specimens were cut longitudinally at 45 and 90 degrees with respect to the longitudinal ribs' plan to measure their geometrical properties, as shown in Fig. 2. The measurements were performed over 10 ribs using high-resolution

Table 1—Geometrical and mechanical properties of reinforcing bars

Type	Parameter	Test bar No. 16 (No. 5)	Test bar No. 19 (No. 6)
Mechanical	Young's modulus, GPa (ksi)	197 (28570)	208 (30170)
	Yield strength at 0.2%, MPa (ksi)	733 (106.3)	475 (68.9)
	Ultimate strength, MPa (ksi)	962 (139.5)	742 (107.6)
	Elongation at rupture, %	10.5	12.7
Geometrical	Nominal diameter d_b, mm (in.)	15.9 (0.63)	19.1 (0.75)
	Core diameter D, mm (in.)	14.8 (0.58)	17.7 (0.70)
	Ribs' height h_r, mm (in.)	0.9 (0.035)	1.3 (0.051)
	Ribs' top width b_r, mm (in.)	1.0 (0.039)	1.2 (0.047)
	Ribs' base width a_r, mm (in.)	4.9 (0.193)	5.6 (0.220)
	Ribs' spacing s_r, mm (in.)	10.8 (0.425)	12.6 (0.496)
	Ribs' face angle θ, degrees	25	30
	Ribs' inclination β, degrees	67	68
	Σ gaps*, mm (in.)	4.0 (0.16)	4.0 (0.16)
	Relative rib area* R_r, adim	0.080	0.100

*Based on Fei et al.[33]

photographs and a CAD software for each longitudinal cut. Table 1 summarizes the mean mechanical and geometrical values from the three and 20 measurements of each bar size, respectively.

Artificial voids

To create the artificial voids, fresh silicone was inserted into hollow plastic tubes and extracted once the silicone had hardened. The resulting tubes were subsequently cut longitudinally into two halves and one piece was then glued over the entire bonded length of the test bars using the same material. To ensure no silicone was deposited elsewhere over the surface of the bars, the position of the voids was defined with masking tape, which was removed once the artificial voids were securely glued in place. Voids of nominal transverse lengths of 10, 20, and 30% of the test bars' perimeter were created and are referred to as unbonded perimeters (u.p.) henceforth. A "top" and "bottom" void configuration, as seen in Fig. 3(a) and (b), respectively, were also studied because, depending on the location of a bar and the direction of the shotcrete flow, voids could be created facing either the exterior or the interior of a reinforced shotcrete element.

Mixture design

Specimens were cast using a prebagged mixture intended for wet-mix shotcrete (maximum aggregate size of 10 mm [0.4 in.]), which was poured into the forms. A constant water-binder ratio (w/b) of 0.45 was used in combination with a polycarboxylate-based water reducer complying with Types A and F categories of the ASTM C494/C494M-16[16] standard. This produced an SCC mixture with which it was possible to properly encase the artificial voids by providing only a minimal amount of external consolidation; only the corners of the forms were carefully tapped a few times. All the forms were filled in two lifts and the first layer was placed in all specimens before the second layer. Because a considerable amount of concrete was placed below the test bars and

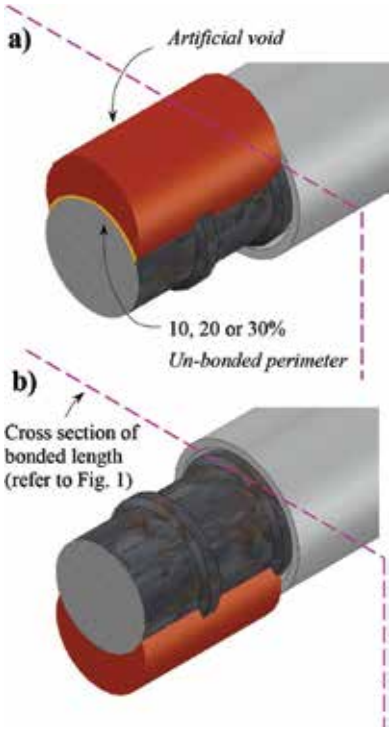

Fig. 3—(a) Top; and (b) bottom position of artificial voids.

a possible bond performance deterioration (additional to the presence of the voids) caused by excessive water accumulation under the test bars was a concern, a family of specimens having a 0.55 w/b mixture was also tested. In that case, no water reducer was added and the consolidation was done in accordance with ASTM C192/C192M-16a.[17] The proportions of both mixtures are shown in Table 2.

Properties of concrete

Cylinders (100 x 200 mm [4 x 8 in.]) were prepared to test the compressive strength f_c,[18] the splitting tensile strength f_s,[19] and the Young's modulus E_c[20] of all the concrete

Table 2—Mixture composition of both types of concrete

Component	w/b = 0.45	w/b = 0.55
Ordinary portland cement, kg/m^3 (lb/yd^3)	393.1 (663)	376.7 (635)
Silica fume, kg/m^3 (lb/yd^3)	34.3 (58)	32.9 (55)
Coarse aggregate 2.5 to 10 mm, kg/m^3 (lb/yd^3)	708.6 (1194)	680.7 (1147)
Sand 0.08 to 5 mm, kg/m^3 (lb/yd^3)	1016.6 (1714)	976.5 (1646)
Water, kg/m^3 (lb/yd^3)	191.2 (322)	224.8 (379)
Air, %	3.4*	2.1*
Water reducer, mL/100 kg of binder (fl. oz./100 lb)	750 (11)	—

*Based on ASTM C231/C231M-14.

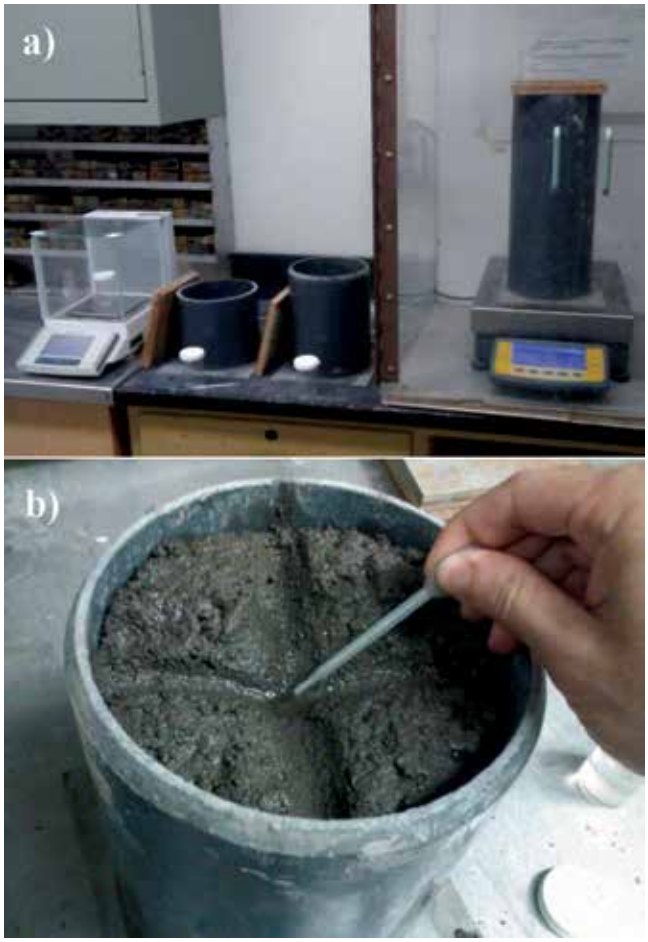

Fig. 4—(a) Equipment needed for bleed test; and (b) bleed water collected from container.

mixtures. The cylinders were cured in the same way (for 1 week using wet burlap) and were tested at the same age as the "beam-end" specimens. Moreover, the slump[21] and the slump flow along with the visual stability index (VSI)[22] were documented for the 0.55 and the 0.45 w/b mixtures, respectively; the air content was also measured for both of them.[23] All tests were performed using the concrete from the second lift, with which the test bar was encased. The bleeding properties of both types of concrete mixtures—that is, their average bleeding rate R and their bleeding capacity ΔH—were quantified following the method proposed by Josserand and de Larrard.[24] The procedure requires three cylindrical containers of different heights (as those shown in Fig. 4(a)) to be filled and to collect the bleed water from the intersection of two orthogonal tracks made on the surface of the concrete (and inclined towards the center) at a regular time interval using a pipet as shown in Fig. 4(b). The bleed water is used to calculate ΔH, which in turn, serves to calculate R (whose values are independent of the container's height) and determine its maximal value R_{max}. During the entire test, the tallest container rests on a 0.1 g (0.04 oz) accurate scale so its weight loss rate can be measured and later considered as the average bleed water evaporation of all the containers. In this investigation, the containers were 150, 210, and 430 mm (5.9, 8.3, and 16.9 in.) tall and had an inner diameter of 150 mm (5.9 in.). Moreover, the concrete was consolidated in the same manner as was done to cast the "beam-end" specimens. This method is advantageous over similar methods such as the ASTM C232/C232M-14[25] standard because the containers do not need to be tilted to collect the bleed water. However, it still provides the opportunity to calculate the bleeding in the same way as the standard does. All the concrete test results are summarized in Table 3.

Testing procedure

The "beam-end" specimens were tested using a 311 MTS frame and the setup shown in Fig. 5. The tests were performed at 0.5 mm/min displacement control and the slip of the reinforcing bars was recorded at the loaded end and at the unloaded end of the test bar using two linear position sensors with return spring on each side. The "beam-end" specimen was lifted using the holes provided by the transversal PVC sleeves and then laid on a steel box anchored to the base of the test frame. After the specimen was pushed with the alignment plate so as to align the test bar with the actuator's longitudinal axis, the specimen was gradually tightened with the compression reaction plate and the tiedown plate. Finally, the pulling device, which consisted of two square shafts pin-holding a thick cylinder with a hole in its middle, was inserted around the test bar. A conical wedge was then placed around the test bar so that the cylinder from the pulling device would bear against it while the bar was tensioned. A detailed description of the testing apparatus and procedure to test ASTM A944-10 "beam-end" specimens is given by Basso Trujillo et al.[26] The properties of the hardened concrete were measured right after the "beam-end" specimens were tested and are presented in Table 3.

Test parameters

Specimens were grouped in families using labels which indicate the size of the test bar (No. 16 [No. 5] or No. 19 [No. 6]), the w/b of the mixture (0.45 or 0.55) and the orientation of the artificial voids (T or B for top and bottom, respectively, and based on Fig. 1 and 3) if they were used. Three replicas were built for each configuration. The 10% u.p. was not tested for the "Bottom" configuration, as early results showed that the bond strength was not significantly reduced in comparison with perfectly encapsulated bars (u.p. = 0%). Considering all of the u.p.'s for each family (13) and the replicas for each one of them (3), a total of 13 x

Table 3—Test results of concrete mixtures

Family	u.p., %				*w/b*	f_c, MPa (psi)	f_s, MPa (psi)	E_c, GPa (ksi)	Air,%	Slump flow, mm (in.) / Slump, mm (in.)	VSI	R_{max}, μm/min (mils/min)	Test*, days
#16-0.45	0	—	—	—	0.45	57.7 (8370)	3.9 (570)	33.3† (4830)	3.4	550 (21.7)	0 ~ 1	2.2‡ (0.1)	24 ± 2
#16-0.45 T	—	10	20	30									
#16-0.45 B	—	—	20	30									
#19-0.45	0	—	—	—									
#19-0.45 T	—	10§	20	30									
#19-0.45 B	—	—	20	30									
#16-0.55	0	—	—	—	0.55	34.7 (5030)	2.5 (360)	25.4 (3680)	2.1	140 (5.5)	—	6.5† (0.3)	8

*In reference to both "beam-end" specimens and mechanical properties of concrete.
† Poisson's ratio of 0.14 was measured at the same time.
‡Mean from three molds of different height and only one mixture.
§Specimens' results were discarded due to malfunction in equipment.

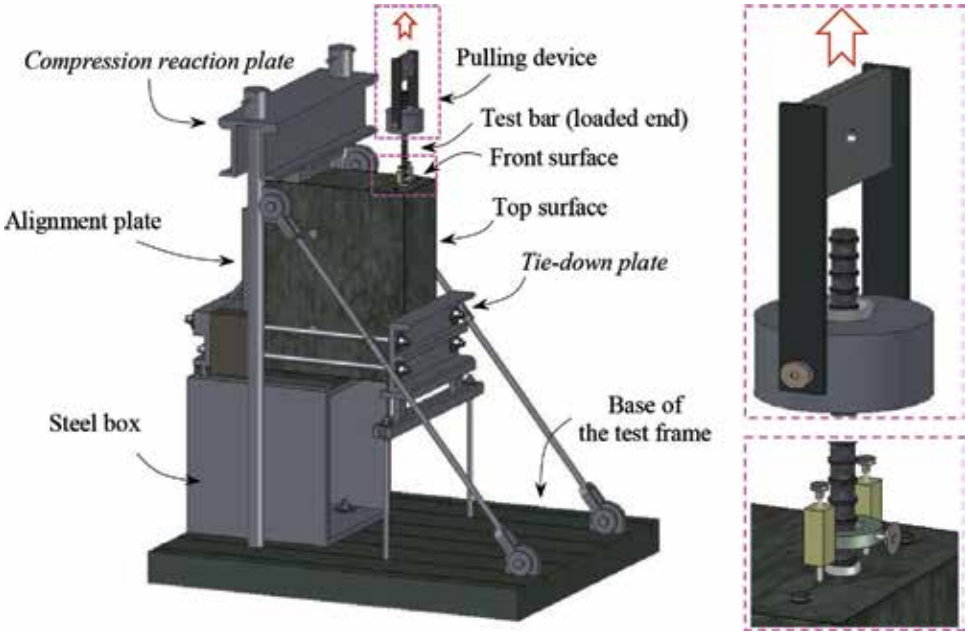

Fig. 5—Test setup of ASTM A944-10 "beam-end" specimen.

3 = 39 "beam-end" specimens were built. However, only the results of 36 of them are presented in the following section, as explained in Table 3.

RESULTS AND DISCUSSION

Stress-slip curves

The measured load *P* has been normalized with respect to the nominal transversal area of the test bars A_b and is plotted against the slip of the bars for the different u.p.'s under study. At the loaded end only, the elastic elongation of the portion of the test bars between the attachment of the linear position sensors and the end of the lead length was subtracted from the measured slip. Moreover, only the test bars with a "top" void configuration and a *w/b* of 0.45 are presented in this section. The curves of the loaded and the unloaded ends are shown in Fig. 6(a) and (b) for the No. 16 (No. 5) test bars and in Fig. 7(a) and (b) for the No. 19 (No. 6) test bars. As expected, the slip associated to the loaded end is larger than the one measured at the unloaded end as the latter captures the "stiffness" of the entire bonded length. The difference between both measures represents the lengthening of the reinforcing bar and its absolute value increases as the bonded length is increased. As can be seen in Fig. 6(a) and (b), a u.p. of 10% causes no apparent change in the overall bond behavior of a bar in comparison to a perfectly encapsulated bar (0% u.p.). Indeed, in both cases, the slope of the ascending curve (referred to as the slip stiffness henceforth), remains constant until the ultimate bond stress (P_{max}/A_b) is attained. Beyond that point, the ribs of the bar crush the concrete in front of them, creating residual stresses as the bar continues to slip relative to the concrete. In all cases, the transition from a 10% to a 30% u.p. causes the slip stiffness to decrease progressively as the ultimate bond stress is attained as can be observed in Fig. 6(a) and (b) as well as in Fig. 7(a) and (b). At a 20% u.p., the ultimate bond stress had been reduced in the range of 3 to 8% and at a 30% u.p. in the range of 20 to 25% relative to perfectly encapsulated test bars.

Despite the fact that the concrete was not actually sprayed, the bond behavior of the specimens provides useful evidence

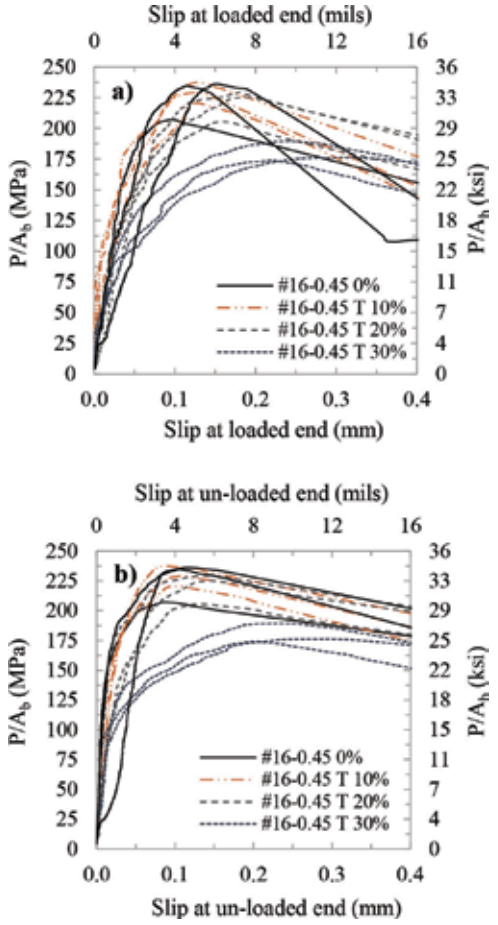

Fig. 6—(a) Stress-slip curves of No. 16 (No. 5) test bars at loaded; and (b) unloaded end.

to define threshold values defining bond behavior changes between specimens with different encapsulation qualities. In reality, according to the investigation of Basso Trujillo et al.[9] in which the bond performance of shotcrete and cast-in-place "pullout" specimens was compared, the slip stiffness of shotcrete specimens would be slightly greater than those shown in Fig. 6(a) and (b) as well as those shown in Fig. 7(a) and (b) due to the high compaction of the concrete obtained upon its impact on the forms. Nonetheless, the ultimate bond stress between both methods of concrete placement should be the same despite the different slip performance. It is for this reason that the ultimate bond stress is used subsequently for the analysis and thus the values obtained with both test bar sizes are plotted in Fig. 8 as a function of the u.p. In general, the ultimate bond stress for different qualities of encapsulation seems to be independent of the tested bar sizes (No. 16 [No. 5] and No. 19 [No. 6]) and the reduction is best characterized by a second-order polynomial regression. This model is both significant (F_0 = 28.89 and p-value < 0.000) and adequate (F_0 = 0.00 and p-value = 1.000) based on an analysis of variance[27] and possesses an adjusted Pearson coefficient (R^2_{adj}) of 0.736.

Size of bars

To support the assertion that the reduction of the ultimate bond stress is independent of the bar size, an equal variance

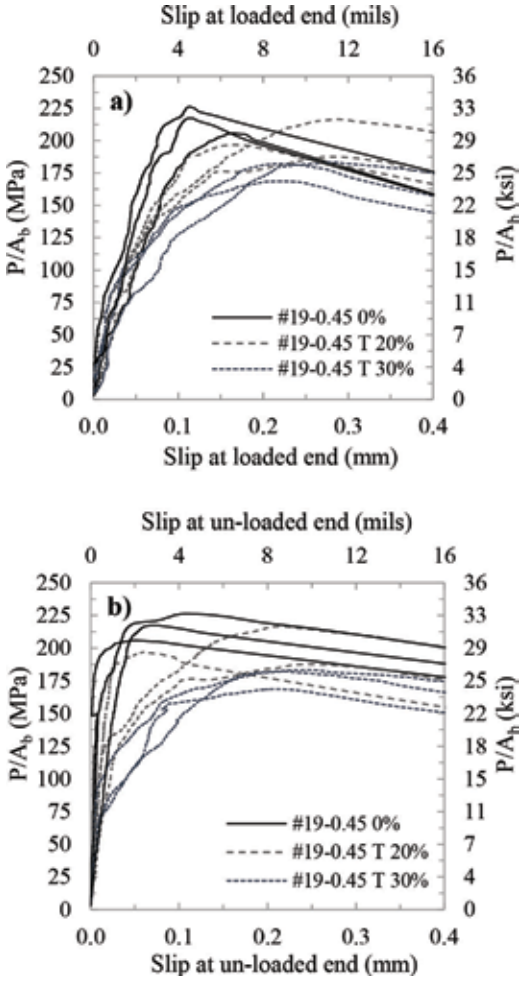

Fig. 7—(a) Stress-slip curves of No. 19 (No. 6) test bars at loaded; and (b) unloaded end.

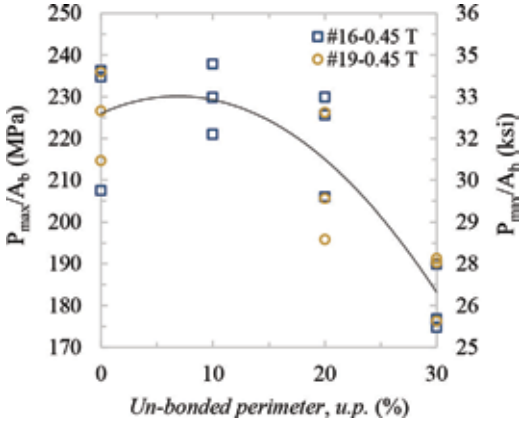

Fig. 8—Effect of u.p. on ultimate bond stress of bars No. 16 (No. 5) and No. 19 (No. 6).

pairwise comparison t-test[27] was performed. This is formally done by defining a null (H_0) and an alternative hypothesis (H_a), as expressed in Eq. (1), to determine if the ultimate bond stresses of the entire population μ_i of specimens with one bar size are equal or not to another one having a different bar size but the same u.p.

$$H_0: \mu_1 = \mu_2 \text{ versus } H_a: \mu_1 \neq \mu_2 \quad (1)$$

The outcome of the test, most frequently expressed with a *p*-value, determines if there is enough evidence to accept H_0 or if it should be rejected. The *p*-value represents the level of risk a decision-maker is willing to take at the moment H_0 is accepted or rejected; a decision based on a *p*-value equal to 0.05 implies taking a risk of 5% to falsely reject H_0. The *p*-value is obtained based on the degrees of freedom *v* associated with the size of the combined sample and the calculated t_0 test-statistic (distributed as *t*) which, in turn, is calculated using the mean of each families' ultimate bond stress (average P_{max}/A_b). In this case, *v* equals $n_1 + n_2 - 2 = 4$, where n_i is the size of each family. When a precise level of risk is established as the threshold to accept or to reject H_0, its value is called the *level of significance* (α) of the test. The results of the comparison based on α = 0.05 are shown in Table 4. Because the resulting *p*-values are greater than any relevant level of significance (α ≤ 0.05) in all cases, there is not sufficient evidence to reject H_0 and thus we can conclude that the ultimate bond stress in the presence of voids is independent of the sizes of the bars tested herein. It is worth noticing that as the u.p. increases, the standard deviation *S* seems to decrease. Indeed, it is mostly due to the variability of the concrete properties that dispersion within specimens occurs and thus the lesser the concrete around the bar, the lesser the standard deviation.

Position of voids

An equal-variance *t*-test was also performed to assess the impact of a void's position on the bond strength of a bar. The comparisons were made between specimens having "top" and "bottom" void configurations but having the same bar size and u.p.'s. The results are shown in Fig. 9 in which the error bars represent one standard deviation away from P_{max}/A_b. The results of the test are presented in Table 5 and, based on the same analysis procedure described previously, the position of the void did not have a significant impact on the ultimate bond stress in most situations. In the case of family No. 16-0.45 30%, the test detected a difference between the population's means. Surprisingly, the mean bond stress of this family with a "bottom" void configuration presented higher values than the one obtained with an u.p. of 20% for the same bar size (208.2 versus 200.4 MPa [30.2 versus 29.1 ksi]); it is for this unexpected and unrealistic difference that the bond stresses of bar sizes No. 16 (No. 5) and No. 19 (No. 6) were not combined for a given u.p. despite the fact that results are independent of the sizes of the bars as described in the previous chapter. Because in all other three cases the results lead to the conclusion that mean bond stresses are equal between "top" and "bottom" void configurations, there is strong evidence that a void facing the surface of a structural element and another of the same size facing its interior would have approximately the same impact on the bond strength of the bar.

Table 4—Equal variance *t*-test results for size of bars

u.p., %	Bar No.	*n*	Average P_{max}/A_b, MPa (ksi)	*S*, MPa (ksi)	t_0	*v*	*p*-value	Result*
0	16	3	226.1 (32.8)	16.2 (2.3)	0.04	4	0.972	Equal
	19	3	225.7 (32.7)	10.7 (1.6)				
20	16	3	220.5 (32.0)	12.8 (1.9)	0.98	4	0.384	Equal
	19	3	209.2 (30.3)	15.5 (2.2)				
30	16	3	180.5 (26.2)	8.2 (1.2)	0.80	4	0.467	Equal
	19	3	185.9 (27.0)	8.4 (1.2)				

*Based on level of significance α = 0.05.

w/b

The visual stability index (VSI) of the 0.45 *w*/*b* mixture resulted mainly in Grade 0 values (refer to Fig. 10) and sporadic Grade 1 values; these observations provided preliminary evidence that the SCC mixture had a very low propensity to bleed. Quantitatively, this was confirmed by

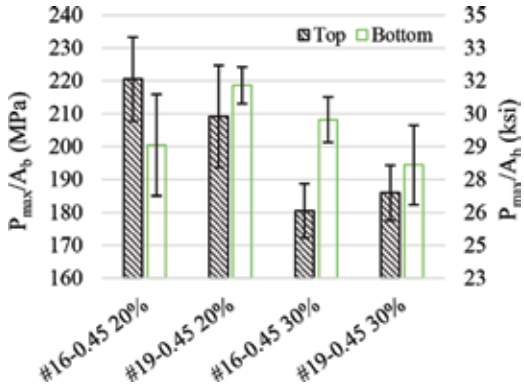

Fig. 9—Ultimate bond stress of bars with different void position.

Table 5—Equal variance *t*-test results for position of voids

Family	Position	u.p., %	n	Average P_{max}/A_b, MPa (ksi)	S, MPa (ksi)	t_0	*v*	*p*-value	Result*
No. 16-0.45	T	20	3	220.5 (32.0)	12.8 (1.9)	1.74	4	0.157	Equal
	B		3	200.4 (29.1)	15.4 (2.2)				
No. 19-0.45	T	20	3	209.2 (30.3)	15.5 (2.2)	1.00	4	0.376	Equal
	B		3	218.6 (31.7)	5.6 (0.8)				
No. 16-0.45	T	30	3	180.5 (26.2)	8.2 (1.2)	4.49	4	0.011	Not Equal
	B		3	208.2 (30.2)	6.9 (1.0)				
No. 19-0.45	T	30	3	185.9 (27.0)	8.4 (1.2)	1.00	4	0.372	Equal
	B		3	194.4 (28.2)	12.1 (1.8)				

*Based on level of significance α = 0.05.

Fig. 10—Typical consistency of 0.45 w/b *ratio mixture showing VSI of 0.*

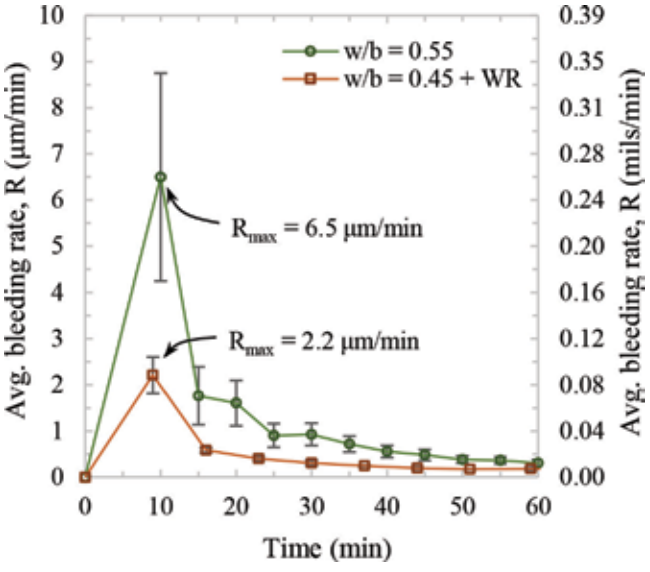

Fig. 11—Average bleeding rate of mixtures. (Note: 1 µm/min = 0.039 mils/min.)

the average bleeding rate R and the bleeding capacity (ΔH) measurements (shown respectively in Fig. 11 and Fig. 12) in comparison with those obtained with the 0.55 *w/b* mixture; in Fig. 11, the error bars represent one standard deviation away from the mean. Only the ΔH of the 430 mm tall container is presented because it represents the approximate height of the concrete below the test bars in the "beam-end" specimens. In addition, the volume of bleed water per unit area V and the accumulated bleed water (bleeding) expressed as a percentage of the mixture's net mixing water of each container are presented in Fig. 12 for both mixtures. Both V and bleeding were calculated based on the ASTM C232/C232M-14[25] standard using the total amount of bleed water collected from the containers before the concrete hardened. As can be observed, the maximum average bleeding rate R_{max} and ΔH were reduced by approximately 66% as the *w/b* was lowered by approximately 20% with the addition of the water reducer. In fact, based on the ASTM C232/C232M-14[25] standard's results (refer to Fig. 12), it can be

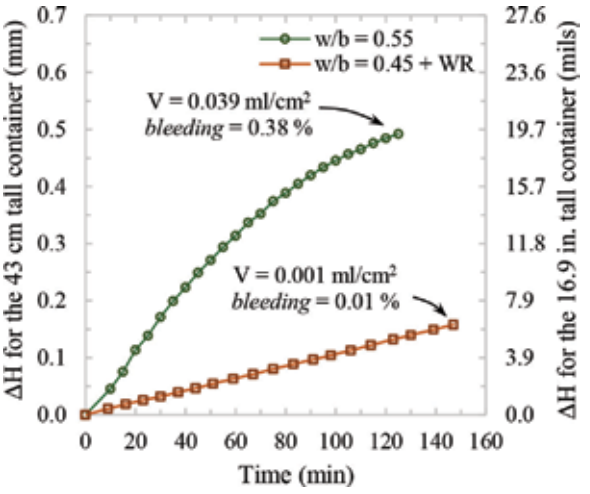

Fig. 12—Bleeding capacity of mixtures. (Note: 1 mL/cm² = 0.218 fl. oz./in.²)

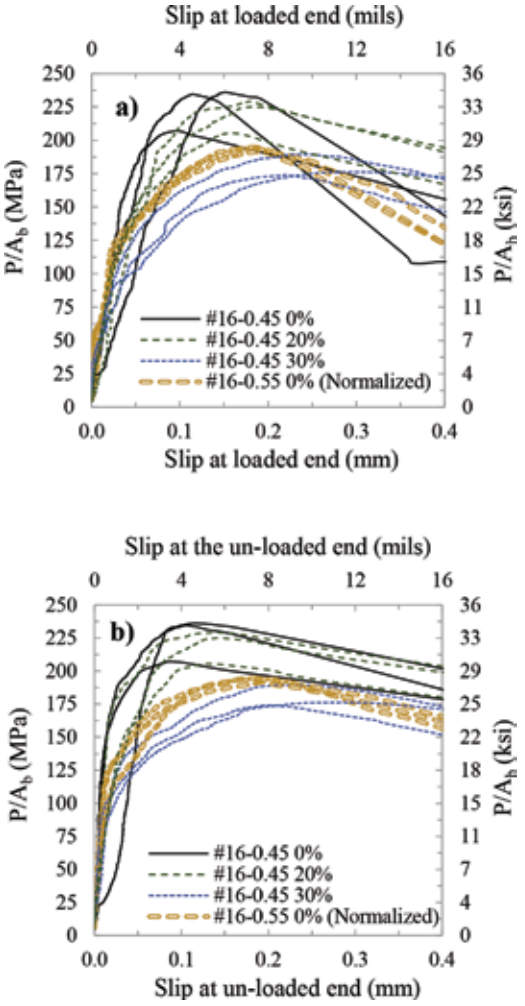

Fig. 13—(a) Stress-slip curves of 0.45 and 0.55 w/b *mixtures at loaded; and (b) unloaded end.*

said that the reduction of the *w/b* produced a mixture with "essentially no bleeding"[28] as the amount of bleeding was 0.01%. In terms of bond strength, the almost complete lack of bleeding produced a superior ultimate bond stress as can be observed in Fig. 13(a) and (b), where the stress-slip response of the "beam-end" specimens belonging to families

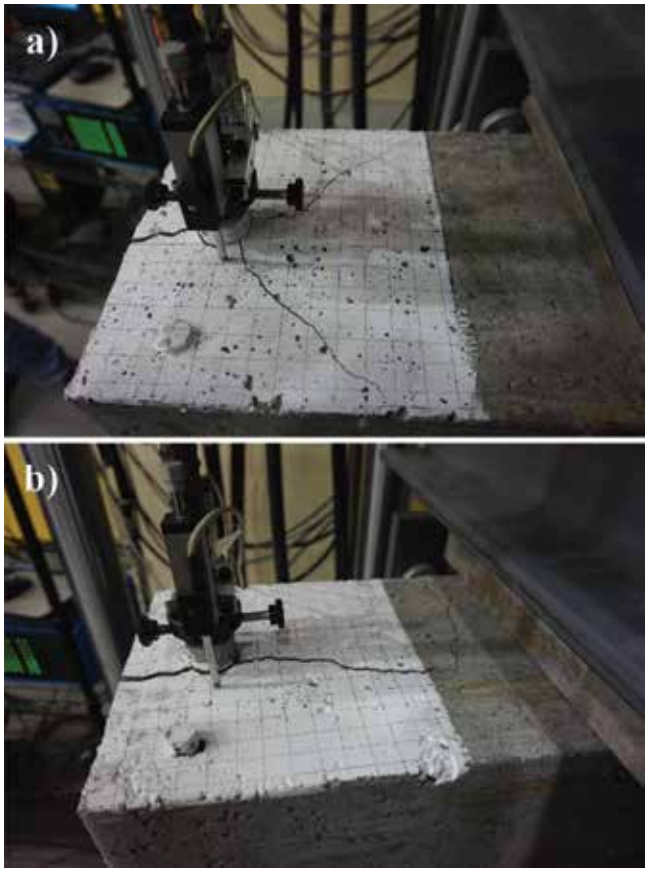

Fig. 14—(a) Y-; and (b) T-shape splitting patterns at front surface (grids are 15 x 15 mm [0.6 x 0.6 in.]).

No. 16-0.45 0%, 20%, 30% and No. 16-0.55 0% are plotted. To properly compare the response of all specimens, the bond stresses of the higher *w*/*b* family were normalized relative to the f_c of the lower *w*/*b* family. Therefore, the bond stresses of the No. 16-0.55 0% family of specimens were multiplied by $(57.7/f_c)^{1/4}$ assuming that the bond strength is proportional to the 1/4 power of the compressive strength. In past research, either a value of 1/2 or 1/4 has been used as a normalization coefficient but it has been shown that the latter is more accurate when f_c is greater than 55 MPa (7.98 ksi)[29-31]. This assured the specimens' response was equivalent in terms of bulk compressive strength with the only difference being the increased porosity around the bar of the specimens cast with a higher *w*/*b* mixture. As can be observed, using a 0.45 *w*/*b* mixture with a water reducer caused the initial branch of the stress-slip curve to have a more or less constant slope, which best approximates the behavior of shotcrete specimens.[9] This effect may be explained due to the possibly lower porosity in the vicinity of the bars obtained with the SCC mixture in comparison to regular concrete,[32] as no internal vibration is necessary with the former type of concrete. Surprisingly, besides the evident difference of the ultimate bond stress between perfectly encapsulated bars (which is strongly linked to the normalization coefficient used), the bond behavior of the bars encased with the 0.55 *w*/*b* was considerably degraded and produced a similar bond to bars having artificial voids in between 20 and 30% u.p.'s. This is extremely relevant because it emphasizes how crucial the properties of the bar-concrete interface are on both shotcrete and cast-in-place concrete and how each effect needs to be addressed with appropriate measures.

Failure mode

All of the specimens (except one) failed by splitting. At the top surface (refer to Fig. 1 and 5), a crack ran parallel and above the test bar and fanned out to the sides after the length of the bonded section of the bar had been passed. At the front surface, two different types of splitting patterns occurred. In the first case (Y-shape pattern), two diagonal cracks grew towards the bottom of the specimen at approximately 120 degrees between one another and with respect to the top surface crack as shown in Fig. 14(a). In the second case (T-shape pattern), one single crack grew towards the bottom of the specimen parallel to the top surface crack and then fanned out towards the sides of the specimen before the compression reaction plate was reached as shown in Fig. 14(b). The two types of splitting patterns were observed on all specimens and no correlation was found between the size of the voids or the family of the specimens. In fact, these two splitting patterns are usual and can even be observed between specimens having a concrete compressive strength difference as low as 2.5 MPa (0.36 ksi).[33] The only specimen with an unusual mode of failure belonged to family No. 16-0.45 T 30%. Initially, it failed by splitting and an initial crack appeared on the top surface of the specimen. However, as loading continued, the crack stopped to grow and the mode of failure transformed into a pullout mode. The crack did not extend all the way towards the end of the bonded length and did not appear on the front surface.

FURTHER RESEARCH

Although the results presented herein are essential to understand the impact of defects on the bond strength of reinforcing bars, the experimental campaign recreated only the "worst-case" scenario in which the defects covered the entire bonded length of the test bars. Thus, it is of vital importance to further explore the impact of "localized voids" (voids covering only a portion of the bonded length of the bar), as this may occur in congested areas of reinforcement or lap splice regions. The impact of the confinement (concrete cover and transverse reinforcement) should also be investigated, as this may influence the failure mode of the specimens. This is of prime importance, as it will allow the establishment of design and evaluation criteria considering not only the u.p. if voids might be created or are observed but also in regard of how frequently they appear in a given structural element or preconstruction panel.

CONCLUSIONS

In this research, artificial voids encased with a low *w*/*b* mixture were used to simulate the types of encasement deficiencies that are sometimes found in reinforced shotcrete elements when congested elements are sprayed in combination with deficient shooting techniques, inadequate mixtures, or when difficult jobsite conditions exist. The methodology not only made it possible to obtain stress-slip curves with similar characteristics to those that have been observed in

shotcrete (due to the insignificant amount of the mixture's bleeding capacity) but also to obtain clear tendencies and a reduced dispersion of the results. Moreover, the results show how the slip stiffness of the stress-slip curves starts to decrease when artificial voids pass from unbonded perimeters of 10 to 20%. In terms of the ultimate bond stress, the values start decreasing at an unbonded perimeter of 20% and are considerably reduced with unbonded perimeters of 30% reaching reduction values of up to 25% in comparison with perfectly encapsulated bars. In addition, the position of the voids (either facing the exterior or the interior of the element) does not seem to have a great impact on the bond strength of the bars for equal void sizes. In terms of the mode of failure, the majority of the specimens failed by splitting in the same manner as has been reported in the literature.[33] Nonetheless, it is believed that voids with an unbonded perimeter larger than 30% might cause the mode of failure to change from splitting to pullout when voids cover the entire bonded length. The results also showed how the impact of voids is as important as the one caused by excessive bleeding in cast-in-place concrete because a bleeding increase of approximately 3 times (from a condition of almost no bleeding) caused a bond behavior similar to the one observed with specimens with artificial voids of unbonded perimeters larger than 20%.

Therefore, based on the results of this investigation and those available in the literature, it seems that actions to counteract the change in the stress-slip behavior and the ultimate bond stress reduction should be considered in the design of reinforced shotcrete structures once voids having unbonded perimeters equal to or larger than 20% are expected. Indeed, unbonded perimeters of approximately 10% u.p. have little impact on the bond performance of a bar in comparison with perfectly encapsulated bars; this holds even in the worst-case scenario in which the length of the voids covered the entire bonded length of the test bar. Unbonded perimeters equal to or larger than 20% should be carefully treated as bigger confinement provided by concrete cover or transverse reinforcement may induce a change in the mode of failure and consequently a brittle behavior of the reinforced concrete elements. It is the hope of the authors that the results can already serve as a solid background to enhance or validate the current evaluation methods intended for shotcrete structures and preconstruction panels. As future work will be completed (the effect of "localized voids", concrete cover, and transverse reinforcement), proper guidelines for the design are intended to be developed.

AUTHOR BIOS

ACI member **Pasquale Basso Trujillo** *is a PhD candidate at Université Laval, Québec, QC, Canada. He is a member of ACI Committee 506, Shotcreting, and Joint ACI-ASCE Committee 408, Bond and Development of Steel Reinforcement. His research interests include shotcrete, mixture proportioning, concrete paving, finite element analysis, and uncertainty in risk assessment.*

Marc Jolin, *FACI, is a Professor in the Department of Water and Civil Engineering at Université Laval. He is Chair of ACI Committee 506, Shotcreting, and Secretary of ACI Subcommittee C601-I, Shotcrete Inspector, and is a member and past Chair of ACI Committee C660, Shotcrete Nozzleman Certification. His research interests include shotcrete, service life, reinforcement encasement quality, admixtures, and rheology of shotcrete.*

Bruno Massicotte, *FACI, is a Professor in the Department of Civil, Geological and Mining Engineering at the École Polytechnique de Montréal, Montreal, QC, Canada. He is a member of ACI Committees 239, Ultra-High-Performance Concrete; 342, Bridge Evaluation; and 544, Fiber-Reinforced Concrete. His research interests include the structural use of fiber-reinforced concretes, bridge analysis, design and assessment, and advanced structural analysis of concrete structures.*

Benoît Bissonnette, *FACI, is a Professor in the Department of Civil and Water Engineering at Université Laval. He is a member of ACI Committees 223, Shrinkage-Compensating Concrete, and 364, Rehabilitation. His research interests include infrastructure rehabilitation, the volumetric behavior of cement materials, cracking, self-leveling concretes, shrinkage-compensating concretes, instrumentation, and development of characterization tests.*

ACKNOWLEDGMENTS

The authors are grateful to the Concrete Infrastructure Research Center (CRIB) of Québec, the Natural Sciences and Engineering Research Council of Canada (NSERC), King Packaged Materials and Co., the Canadian Council of Independent Laboratories (CCIL), The American Shotcrete Association (ASA) and the Québec and East Ontario Chapter of the American Concrete Institute (ACI) for their financial support. Furthermore, special thanks are extended to J.-D. Lemay and M. Thomassin-Mailhot (research engineers), to R. Malo (expert laboratory technician) and to P.-A. Tremblay and A. Melançon (laboratory technicians) of the Department of Civil and Water Engineering at Université Laval for their outstanding work and support during the casting and the testing operations.

NOTATION

A_b	=	nominal cross-sectional area of reinforcing bar
a_r	=	base width of reinforcing bar's ribs
b_r	=	top width of reinforcing bar's ribs
β	=	angle of reinforcing bar's ribs relative to longitudinal axis of bar
D	=	core diameter of reinforcing bar
d_b	=	nominal diameter of reinforcing bar
E_c	=	concrete's elastic Young's modulus at day of testing
F_0	=	F-statistic calculated from sample
f_c	=	compressive strength of concrete at day of testing
f_s	=	splitting strength of concrete at day of testing
H_0	=	null hypothesis of pairwise comparison test method
H_a	=	alternative hypothesis of pairwise comparison method
h_r	=	height of reinforcing bar's ribs
n	=	number of specimens tested per family
P	=	measured load
P_{max}	=	measured ultimate load
p-value	=	smallest level of significance that would lead to rejection of null hypothesis
R	=	average bleeding rate
R_{max}	=	maximum average bleeding rate
R_r	=	relative rib area
R^2_{adj}	=	adjusted Pearson coefficient of regression
S	=	standard deviation
s_r	=	spacing between reinforcing bar's ribs
t_0	=	t-statistic calculated from sample
v	=	degrees of freedom of pairwise comparison test method
α	=	level of significance of statistical comparison test
ΔH	=	bleeding capacity
μ_i	=	population of sample
θ	=	face angle of reinforcing bar's ribs

REFERENCES

1. Warner, J., "Understanding Shotcrete—Structural Applications," *Concrete International*, V. 17, No. 10, Oct. 1995, pp. 55-61.

2. Townsend, F. E. III, "Northern Boulevard Crossing Tunnel CQ039," *Shotcrete*, V. 18, No. 1, Winter 2016, pp. 34-36.

3. Davis, B., "Holcim New Zealand Cement Terminal," *Shotcrete*, V. 19, No. 1, Winter 2017, pp. 26-30.

4. Panian, L.; Steyer, M.; and Tipping, S., "Post-Tensioned Shotcrete Shearwalls," *Concrete International*, V. 29, No. 10, Oct. 2007, pp. 39-45.

5. Townsend, F. E. III, "The Plaza Substation And Queen Structures," *Shotcrete*, V. 18, No. 1, Winter 2016, pp. 22-23.

6. ACI Committee 506, "Visual Shotcrete Core Quality Evaluation (ACI 506.6T-17)," American Concrete Institute, Farmington Hills, MI, 2017, 4 pp.

7. ACI Committee 318, "Building Code Requirements for Structural Concrete (ACI 318-14) and Commentary (ACI 318R-14)," American Concrete Institute, Farmington Hills, MI, 2014, 520 pp.

8. CSA A23.3-14, "Design of Concrete Structures," Canadian Standards Association, Mississauga, ON, Canada, 2014, 297 pp.

9. Basso Trujillo, P.; Jolin, M.; Massicotte, B.; and Bissonnette, B., "Bond Strength of Reinforcing Bars Encased with Shotcrete," *Construction and Building Materials*, V. 169, 2018, pp. 678-688. doi: 10.1016/j.conbuildmat.2018.02.218

10. ASTM A944-10, "Standard Test Method for Comparing Bond Strength of Steel Reinforcing Bars to Concrete Using Beam-End Specimens," ASTM International, West Conshohocken, PA, 2010, 4 pp. https://doi.org/10.1520/A0944-10R1510.1520/A0944-10R15

11. Joint ACI-ASCE Committee 408, "Bond and Development of Straight Reinforcing Bars in Tension (ACI 408R-03)," American Concrete Institute, Farmington Hills, MI, 2003, 49 pp.

12. Orangun, C. O.; Jirsa, J. O.; and Breen, J. E., "The Strength of Anchor Bars: A Reevaluation of the Test Data on Development Length and Splices," University of Texas at Austin, Austin, TX, 1975, 78 pp.

13. Jirsa, J. O.; Lutz, L. A.; and Gergely, P., "Rationale for Suggested Development, Splice, and Standard Hook Provisions for Deformed Bars in Tension," *Concrete International*, V. 1, No. 7, July 1979, pp. 47-61.

14. ASTM A615-16, "Standard Specification for Deformed and Plain Carbon-Steel Bars for Concrete Reinforcement," ASTM International, West Conshohocken, PA, 2016, 7 pp. https://doi.org/10.1520/A0615_A0615M-1610.1520/A0615_A0615M-16

15. ASTM A370-17, "Standard Test Methods and Definitions for Mechanical Testing of Steel Products," ASTM International, 2017, 49 pp. https://doi.org/10.1520/A0370-1710.1520/A0370-17

16. ASTM C494/C494M-17, "Standard Specification for Chemical Admixtures for Concrete," ASTM International, 2017, 10 pp. https://doi.org/10.1520/C0494_C0494M-1710.1520/C0494_C0494M-17

17. ASTM C192/C192M-16a, "Standard Practice for Making and Curing Concrete Test Specimens in the Laboratory," ASTM International, 2016, 8 pp. https://doi.org/10.1520/C0192_C0192M-16A10.1520/C0192_C0192M-16A

18. ASTM C39/C39M-17a, "Standard Test Method for Compressive Strength of Cylindrical Concrete Specimens," ASTM International, West Conshohocken, PA, 2017, 8 pp. https://doi.org/10.1520/C0039_C0039M-17B10.1520/C0039_C0039M-17B

19. ASTM C496-11, "Standard Test Method for Splitting Tensile Strength of Cylindrical Concrete Specimens," ASTM International, West Conshohocken, PA, 2011, 5 pp. https://doi.org/10.1520/C0496_C0496M-1110.1520/C0496_C0496M-11

20. ASTM C469-14, "Standard Test Method for Static Modulus of Elasticity and Poisson's Ratio of Concrete in Compression," ASTM International, West Conshohocken, PA, 2014, 5 pp. https://doi.org/10.1520/C0469_C0469M10.1520/C0469_C0469M

21. ASTM C143/C143M-15a, "Standard Test Method for Slump of Hydraulic-Cement Concrete," ASTM International, 2015, 4 pp. https://doi.org/10.1520/C0143_C0143M-15A10.1520/C0143_C0143M-15A

22. ASTM C1611-14, "Standard Test Method for Slump Flow of Self-Consolidating Concrete," ASTM International, West Conshohocken, PA, 2014, 6 pp. https://doi.org/10.1520/C1611_C1611M-1410.1520/C1611_C1611M-14

23. ASTM C231/C231M-17, "Standard Test Method for Air Content of Freshly Mixed Concrete by the Pressure Method," ASTM International, West Conshohocken, PA, 2017, 9 pp. https://doi.org/10.1520/C0231_C0231M-17A10.1520/C0231_C0231M-17A

24. Josserand, L., and de Larrard, F., "A Method for Concrete Bleeding Measurement," *Materials and Structures*, V. 37, No. 10, 2004, pp. 666-670. doi: 10.1007/BF02480511

25. ASTM C232-14, "Standard Test Method for Bleeding of Concrete," ASTM International, West Conshohocken, PA, 2014, 3 pp. https://doi.org/10.1520/C0232_C0232M10.1520/C0232_C0232M

26. Basso Trujillo, P.; Malo, R.; and Jolin, M., "Alternative Set-Up Apparatus to Test ASTM A944-10 Beam-End Specimens," *Journal of Testing and Evaluation*, V. 46, No. 4, 2018. https://doi.org/10.1520/JTE20170645

27. Montgomery, C. D., *Design and Analysis of Experiments*, seventh edition, 2009.

28. ASTM International, "Significance of Tests and Properties of Concrete and Concrete-Making Materials," 2006, 664 pp. https://doi.org/10.1520/STP169D-EB10.1520/STP169D-EB

29. Darwin, D.; Zuo, J.; Tholen, M. L.; and Idun, E. K., "Development Length Criteria for Conventional and High Relative Rib Area Reinforcing Bars," *ACI Structural Journal*, V. 93, No. 3, May-June 1996, pp. 347-359. doi: 10.14359/9694

30. Zuo, J., and Darwin, D., "Splice Strength of Conventional and High Relative Rib Area Bars in Normal And High-Strength Concrete," *ACI Structural Journal*, V. 97, No. 4, July-Aug. 2000, pp. 630-641. doi: 10.14359/7428

31. Miller, G. G.; Kepler, J. L.; and Darwin, D., "Effect of Epoxy Coating Thickness on Bond Strength of Reinforcing Bars," *ACI Structural Journal*, V. 100, No. 3, May-June 2003, pp. 314-320. doi: 10.14359/12606

32. Salem, H. M., and Maekawa, K., "Pre- and Postyield Finite Element Method Simulation of Bond of Ribbed Reinforcing Bars," *Journal of Structural Engineering*, ASCE, V. 130, No. 4, 2004, pp. 671-680. doi: 10.1061/(ASCE)0733-9445(2004)130:4(671)

33. Brettmann, B. B.; Darwin, D.; and Donahey, R. C., "Bond of Reinforcement to Superplasticized Concrete," *ACI Journal Proceedings*, V. 83, No. 1, Jan.-Feb. 1986, pp. 98-107. doi: 10.14359/1743